



HAL
open science

Lightning remagnetization of the Vredefort impact crater: No evidence for impact-generated magnetic fields

Laurent Carporzen, Benjamin P. Weiss, Stuart A. Gilder, Anne Pommier,
Rodger J. Hart

► To cite this version:

Laurent Carporzen, Benjamin P. Weiss, Stuart A. Gilder, Anne Pommier, Rodger J. Hart. Lightning remagnetization of the Vredefort impact crater: No evidence for impact-generated magnetic fields. *Journal of Geophysical Research*, 2012, 117, pp.1-14. 10.1029/2011JE003919 . insu-03583381

HAL Id: insu-03583381

<https://insu.hal.science/insu-03583381>

Submitted on 22 Feb 2022

HAL is a multi-disciplinary open access archive for the deposit and dissemination of scientific research documents, whether they are published or not. The documents may come from teaching and research institutions in France or abroad, or from public or private research centers.

L'archive ouverte pluridisciplinaire **HAL**, est destinée au dépôt et à la diffusion de documents scientifiques de niveau recherche, publiés ou non, émanant des établissements d'enseignement et de recherche français ou étrangers, des laboratoires publics ou privés.

Copyright

Lightning remagnetization of the Vredefort impact crater: No evidence for impact-generated magnetic fields

Laurent Carporzen,^{1,2} Benjamin P. Weiss,¹ Stuart A. Gilder,³ Anne Pommier,^{1,4}
and Rodger J. Hart⁵

Received 3 August 2011; revised 24 October 2011; accepted 17 November 2011; published 26 January 2012.

[1] The Vredefort impact crater in South Africa is one of the oldest and largest craters on Earth, making it a unique analog for planetary basins. Intense and randomly oriented remanent magnetization observed in surface samples at Vredefort has been attributed to impact-generated magnetic fields. This possibility has major implications for extraterrestrial paleomagnetism since impact-generated fields have been proposed as a key alternative to the dynamo hypothesis for magnetization on the Moon and asteroids. Furthermore, the presence of single-domain magnetite found along shock-generated planar deformation features in Vredefort granites has been widely attributed to the 2.02 Ga impact event. An alternative hypothesis is that the unusual magnetization and/or rock magnetic properties of Vredefort rocks are the products of recent lightning strikes. Lightning and impact-generated fields can be distinguished by measuring samples collected from below the present surface. Here we present a paleomagnetic and rock magnetic study of samples from two 10 m deep vertical boreholes. We show that the magnetization at depth is consistent with a thermoremanent magnetization acquired in the local geomagnetic field following the impact, while random, intense magnetization and some of the unusual rock magnetic properties observed in surface rocks are superficial phenomena produced by lightning. Because Vredefort is the only terrestrial crater that has been proposed to contain records of impact-generated fields, this removes a key piece of evidence in support of the hypothesis that paleomagnetism of the Moon and other extraterrestrial bodies is the product of impacts rather than past core dynamos.

Citation: Carporzen, L., B. P. Weiss, S. A. Gilder, A. Pommier, and R. J. Hart (2012), Lightning remagnetization of the Vredefort impact crater: No evidence for impact-generated magnetic fields, *J. Geophys. Res.*, *117*, E01007, doi:10.1029/2011JE003919.

1. Introduction

[2] The Vredefort structure in South Africa is the eroded remnant of the central uplift zone of a ~300 km diameter impact crater that formed 2.02 billion years (Gyr) ago [Gibson and Reimold, 2002; Reimold and Gibson, 1996]. The central part of the complex multiring crater consists of a ~40 km diameter circular area of Archean basement rocks (Figure 1). Updoming following the impact and subsequent erosion of the top several kilometers have exposed this now steeply dipping section of continental crust [Hart *et al.*, 1990;

Slawson, 1976; Tredoux *et al.*, 1999]. From the crater's center outward, Archean granulites are surrounded successively by charnockytes, gneiss, granite, and a nonconformity overlain by 2.7 Gyr old Witwatersrand Supergroup sediments. U/Pb radiometric ages of the Vredefort basement rocks are as old as 3.5 Ga but show evidence for regional metamorphic events up to 3.0 Gyr ago [Hart *et al.*, 1999; Hart *et al.*, 2004; Moser *et al.*, 2001; Perchuk *et al.*, 2002].

[3] Granitoid rocks from across the central dome have been found to contain very intense, randomly oriented natural remanent magnetization (NRM). The NRM typically has extremely high efficiency (e.g., is not far from saturation), as indicated by a high Koenigsberger (Q) ratio, defined as the NRM intensity (in A/m) normalized to magnetization induced by Earth's field (given by bulk susceptibility in SI units multiplied by 23.87 A/m) [Carporzen *et al.*, 2005; Jackson, 1982; Salminen *et al.*, 2009]. In comparison, impact melt rocks (granophyre dykes and pseudotachylites [Kamo *et al.*, 1996; Koeberl *et al.*, 1996]), were found to be dominantly coherently magnetized in the direction of the known geomagnetic field for the Kaapvaal craton around the time of the impact and have lower Q ratios. Furthermore, the paleomagnetic directions of the melt rocks are consistent with the

¹Department of Earth, Atmospheric, and Planetary Sciences, Massachusetts Institute of Technology, Cambridge, Massachusetts, USA.

²Équipe de paléomagnétisme, Institut de Physique du Globe de Paris, Sorbonne Paris Cité, University of Paris VII-Denis Diderot, UMR 7154 CNRS, Paris, France.

³Department of Earth and Environmental Sciences, Ludwig Maximilians University, Munich, Germany.

⁴Now at School of Earth and Space Exploration, Arizona State University, Tempe, Arizona, USA.

⁵iThemba Labs, Johannesburg, South Africa.

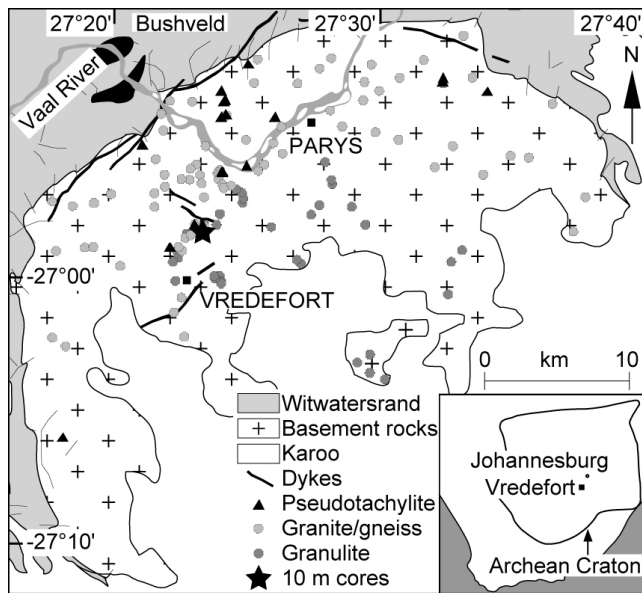


Figure 1. Simplified geologic map of the Vredefort crater [after Nel, 1927] showing the locality of the 10 m deep cores (black star) and paleomagnetic surface sampling sites (light gray and dark gray circles for basement rocks and black triangles for pseudotachylites). From the center of the circular geometry, Archean granulites are surrounded by gneiss and granite and finally 2.7 Gyr old Witwatersrand sediments. Granophyre dykes are represented by bold lines. The southeast part of the circular structure is covered by Mesozoic Karoo sediments. The towns of Vredefort and Parys are shown with black squares.

orientation and intensity of large-scale negative geomagnetic anomalies [Henkel and Reimold, 1998, 2002; Jackson, 1982; Muondjua et al., 2007]. Carporzen et al. [2005] suggested that small-wavelength magnetic fields generated from shock-related plasma that penetrated well below the crater surface could have produced the widely varying magnetization directions in the granitoids, whereas the melt rocks recorded the Earth's ambient field during slow cooling following dissipation of the plasma. If correct, the granitoid paleomagnetism would be the first identified natural terrestrial record of impact-generated magnetic fields. Such fields have been proposed as a key alternative to core dynamos for the magnetization of rocks on extraterrestrial bodies [Hood and Artemieva, 2008; Weiss et al., 2010].

[4] However, the random orientation and very high magnetization efficiency observed for the Vredefort granitoids are commonly observed in Archean and other ancient terranes, where it has usually been ascribed to multiple, overlapping remagnetization events from cloud-to-ground lightning strikes [Biggin et al., 2011; Strik et al., 2003]. Furthermore, Salminen et al. [2009] also observed scattered magnetization directions and high Q values in granitoid rocks outside the Vredefort ring. These observations suggest that the intense, random NRM at Vredefort may not be impact-related, but is rather an artifact of recent lightning strikes. Consistent with the latter possibility is that the estimated postshock temperatures for nearly all of the Vredefort granitoid rocks with random, intense NRM measured by

Carporzen et al. [2005] range from 500 to $>800^{\circ}\text{C}$ [Gibson, 2002], which should have nearly to completely remagnetized any impact plasma-produced remanence during subsequent slow cooling [Salminen et al., 2009].

[5] Lightning produces peak currents up to hundreds of kA lasting for a few tens of milliseconds, thereby generating a strong, circular magnetic field whose axis is oriented perpendicular to the current direction. The current flows nearly orthogonally to the ground surface near the strike location [Sakai et al., 1998; Tauxe et al., 2003; Verrier and Rochette, 2002], but typically assumes a shallower angle as it runs outward near the ground surface [Appel et al., 2006; Beard et al., 2009; Graham, 1961; Sakai et al., 1998; Shimizu et al., 2007]. The intensity of the magnetic field decreases approximately as an inverse function of distance from the current line. This field will produce a secondary isothermal remanent magnetization (IRM) overprint in nearby ground materials. This "lightning induced remanent magnetization" (LIRM) is characterized by high efficiency as indicated by two measures: it has high Q and has remanent magnetization (REM) values (defined as the ratio of NRM to saturation IRM) [Kletetschka et al., 2004] approaching 1 [Appel et al., 2006; Graham, 1961; Sakai et al., 1998; Tauxe et al., 2003; Verrier and Rochette, 2002].

[6] Lightning remagnetized terrains can generate long-lived crustal magnetic fields with gradients of up to several tens of nT/m extending laterally from a few to several tens of meters [Appel et al., 2006; Beard et al., 2009; Graham, 1961; Maki, 2005; Sakai et al., 1998; Shimizu et al., 2007; Tauxe et al., 2003; Verrier and Rochette, 2002]. Repeated lightning strikes on a surface at different locations can build up complex, multicomponent magnetization as the field at any location varies widely in intensity and direction over time. Furthermore, LIRM can remagnetize grains with very high magnetic coercivities. For example, Verrier and Rochette [2002] found that lightning-struck samples affected the coercivity spectrum of natural samples up to hundreds of mT. Lightning can also heat and even melt the materials it strikes. Because of the $\sim 10^9$ J energy released by a lightning strike, temperatures in the surrounding air have been reported to rise up to 30,000 K, while ground temperatures can rise up to 2000 K [Appel et al., 2006; Carter et al., 2010; Essene and Fisher, 1986; Frenzel et al., 1989; Jones et al., 2005].

[7] Archean magnetite in Vredefort granitoid basement rocks commonly lies within the multidomain (MD) size range [Cloete et al., 1999]. In addition, pseudo-single-domain (PSD) to MD magnetite grains (1–200 μm in size) have been observed within brecciated biotite and might have been formed by breakdown of the latter following passage of the shock wave [Nakamura et al., 2010]. A third population of magnetite grains was observed within planar deformation features (PDFs) in Vredefort quartz [Cloete et al., 1999]. The PDFs formed as a result of shock pressures >5 –10 GPa [Gibson and Reimold, 2005; Grieve et al., 1996]. It was proposed that single-domain-sized (SD) magnetite grains along the PDFs resulted from micromelts formed during the impact event that were injected along the PDFs and other microcracks shortly after uplift [Cloete et al., 1999; Hart et al., 1995]. These SD and/or PSD magnetites smaller than 15 μm may also be responsible for a low temperature (~ 102 K) Verwey transition observed in shocked Vredefort granitoids by Carporzen et al. [2006]. The high

magnetization efficiency of SD and/or PSD magnetite grains means their contribution to the NRM could dominate over that from the Archean MD magnetite grains.

[8] Previous paleomagnetic studies have shown that lightning remagnetization typically extends ~ 1 to several meters below the surface [Graham, 1961]. Therefore, if the random intense NRM at the surface was produced by lightning, at depth it should be replaced with low-intensity NRM oriented in a direction parallel to the 2 Ga geomagnetic field. By comparison, because the present erosional surface at Vredefort was at least several km below the original crater bottom [Henkel and Reimold, 1998], the impact plasma hypothesis predicts that rocks both at the present surface and at several meters present-day depth should have similar random intense magnetizations. Therefore, a clear way to distinguish between lightning and impact-related fields is to measure the paleomagnetism of samples collected several meters below the present erosional surface at Vredefort.

[9] With this test as a goal, we drilled two 10 m deep cores in a locality of strong crustal field gradients (over 10,000 nT/m) and intense NRM with scattered directions (Figure 1). The outcrop is relatively flat, with no soil cover except a few lichen patches, and surrounded by grassy soils; the closest tree is about 10 m tall and at about 70 m distance. We mapped the magnetic field of the drilling area using a three axis fluxgate magnetometer at three different altitudes of 0.55, 1.20 and 2.55 m. We also acquired 100 surface samples (2.5 cm diameter by 5–10 cm deep cores) for paleomagnetic measurements in a square grid of using a gas-powered drill.

[10] In addition to studying this locality, we measured paleomagnetic surface samples of granite, gneiss, granulite, and pseudotachylite from 136 surface sites around Vredefort (Figure 1). The latter nearly triples the number of samples discussed by Carporzen *et al.* [2005], yielding 324 new samples from 268 new cores.

2. Sampling and Experiments

2.1. Surface Sampling

[11] The 100 standard paleomagnetic cores were drilled every 1 m in a regularly spaced 9×9 m² grid (black dots in Figure 2a) in granulite with a pronounced vertical metamorphic foliation. We orientated each core with both sun and magnetic compasses using a Pomeroy orientation device at a height of ~ 55 cm above the surface. GPS was used to determine the geographic orientation of the grid (Figure 2a). We observed large declination anomalies (angle between magnetic and geographic north) with orientations scattered widely in azimuth, implying that north cannot be determined accurately using a magnetic compass. We measured the NRM of 100 standard paleomagnetic specimens (2.2 cm high by 2.5 cm in diameter) cut from the 100 cores using a JR-5 spinner magnetometer in the magnetically shielded room at the Institut de Physique de Globe de Paris (IPGP). We also measured the bulk magnetic susceptibility of each sample with an AGICO KLY-3 Kappabridge.

[12] Including the samples reported by Carporzen *et al.* [2005], here we discuss measurements of a total of 319 standard paleomagnetic samples taken from 268 cores of granite, gneiss, and granulite at 110 surface outcrop sites. Each site was at least several tens of meters away from the

closest outcropping pseudotachylite vein, network or dyke (dots in Figure 1). In addition, we sampled 165 cores from 26 sites (triangles in Figure 1) in pseudotachylites and the surrounding granite, gneiss or granulite host rocks from within a few centimeters of these pseudotachylites. Of those 26 sites, 13 were sampled in quarry walls or recently excavated surfaces in quarries, while the other 13 were drilled in surface outcrops. One to three subsamples were taken from each of the 165 cores for a total of 204 pseudotachylite and host rock samples.

2.2. Geomagnetic Surveys

[13] We measured the vector magnetic field ~ 55 cm above each paleomagnetic borehole using a three axis fluxgate magnetometer mounted on the Pomeroy orientation table (estimated orientation uncertainty $< 1^\circ$) (Figure 2a). We also performed two sets of geomagnetic measurements at elevations of 1.2 and 2.55 m over a laterally extended area of 13×13 m² in 1 m intervals centered above the 0.55 m survey (Figure 2a). Finally, we used a Geometrics cesium scalar magnetometer to extend the survey of the total magnetic field along 30 m lines spaced ~ 1 m apart at a height of 2.55 m (Figure 2b).

[14] To obtain the crustal anomaly field (arrows in Figure 2a), we subtracted each component of the International Geomagnetic Reference Field (IGRF) (intensity 28,174.9 nT with geographic orientation of -18.604° declination and -63.76° inclination) from each orientated measurement. In several locations, the intensity of the IGRF was less than half that of the local crustal field (Figure 2a).

2.3. Ten Meter Deep Drilling

[15] The 10 m deep, 2.5 cm diameter drill cores named VRED2 and VRED3 were acquired at two sites ~ 5 m apart using a Winkie drill (an earlier attempt to drill a nearby VRED1 core was abandoned). VRED2 lies within a strong negative geomagnetic anomaly (positive inclination, downward) while VRED3 lies in a strong positive geomagnetic anomaly. VRED2 and VRED3 have hade (angles from vertical/the complements of the dip angles) of 13° and 11° , dipping toward 209.3° and 216.4° , respectively. We paused drilling of each borehole after the first ~ 5 cm without breaking the core in order to orient each core. We then drilled two semicontinuous cores of length 10.12 and 10.56 m, each consisting of 12 and 11 unbroken and coherently oriented segments, respectively. All of these sections are absolutely oriented in inclination, but only the top 0.8 and 1.8 m of the VRED2 and VRED3 cores, respectively, are absolutely oriented in declination because breaks between lower core sections prevented azimuthal orientation.

2.4. Sample Preparation and Experimental Procedure

[16] We prepared 722 subsamples from along the entire lengths of both cores (366 from VRED2 core and 356 from VRED3 core). Small (1–10 cm) consecutive core pieces were also selected to test whether the declination orientation was preserved across breaks. We also sampled regions around the core breaks in order to test for remagnetization during friction and grinding between core sections.

[17] The samples were measured on an automated sample handling system [Kirschvink *et al.*, 2008] integrated with a 2G Enterprises Superconducting Rock Magnetometer

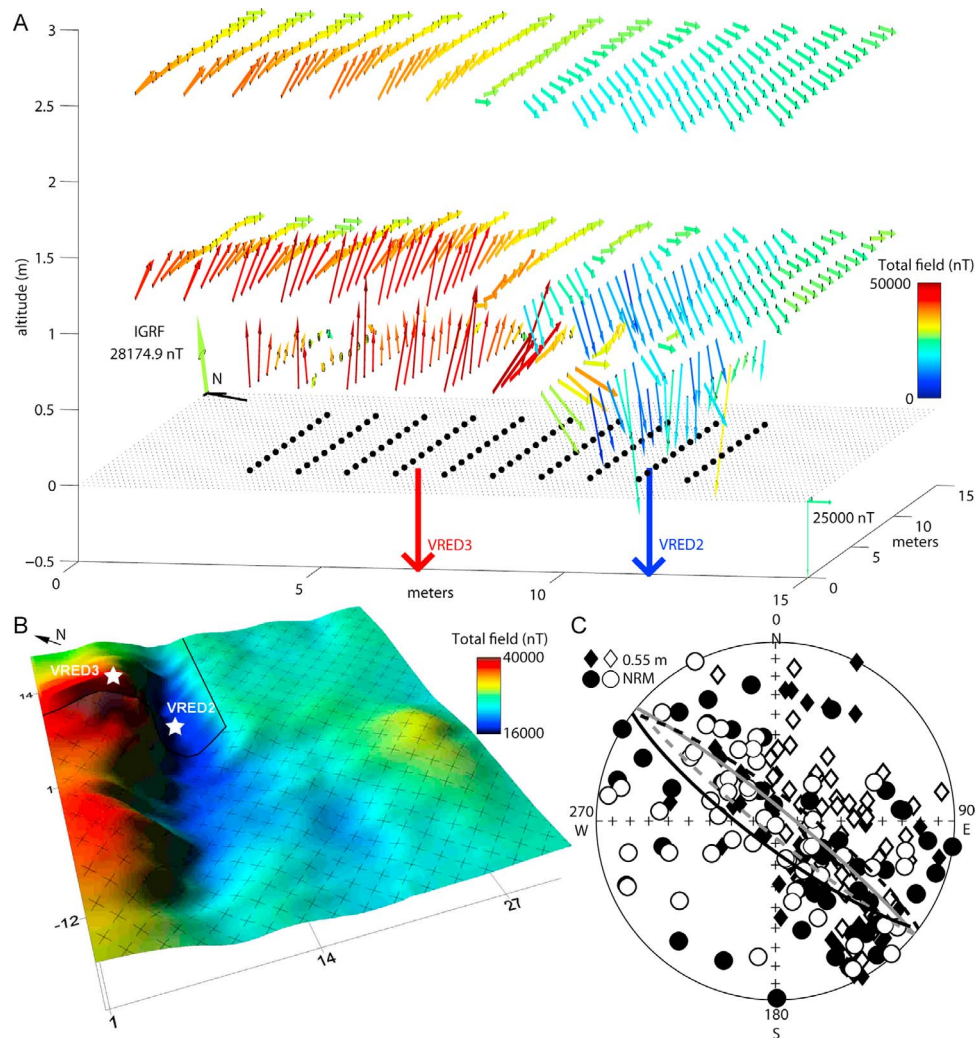


Figure 2. Geomagnetic survey of the 10 m drill core locality in the Vredefort crater. (a) Scaled geomagnetic anomaly vectors (resultant field after vector subtraction of the International Geomagnetic Reference Field) at each location above surface samples (black dots). Colors correspond to the total field intensity. Black dots represent the locations for the 100 surface paleomagnetic cores (~ 5 cm deep). Blue and red vertical arrows extending below ground show the position of the two >10 m deep cores VRED2 and VRED3, respectively. The outcrop has a well-pronounced metamorphic foliation trending $\sim 315^\circ\text{N}$. (b) Cesium scalar magnetometer survey at a height of ~ 2.5 m showing anomaly field variations of up to 20,000 nT over a lateral distance of 30 m. The vertical axis represents the total field intensity. In the north corner, square without crosses shows the $13 \times 13 \text{ m}^2$ area covered by the combined paleomagnetic and geomagnetic survey shown in Figure 2a. White stars show the position of the two >10 m deep cores. Horizontal axes are in meters. (c) Equal area stereonet showing the natural remanent magnetization (NRM) directions of the 100 surface samples (circles) and the directions of the geomagnetic anomaly vectors (diamonds) at 0.55 m altitude. Black and gray great circles correspond to least squares fits of geomagnetic and NRM data, respectively. Solid symbols correspond to lower hemisphere; open symbols and dashed lines correspond to upper hemisphere.

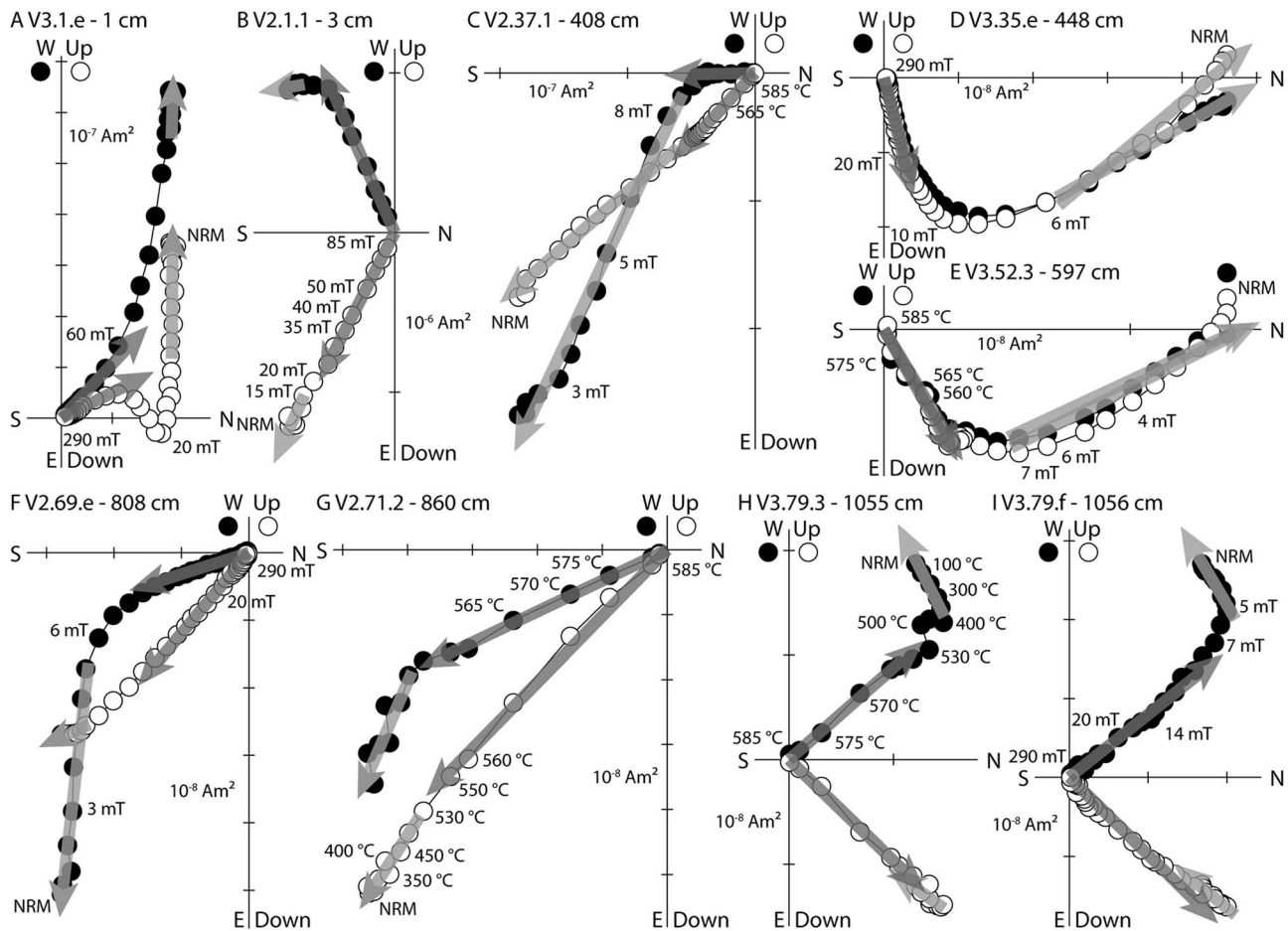


Figure 3. Representative alternating field (AF) and thermal demagnetization of samples from the two >10 m deep cores. Shown in core coordinate system is a two-dimensional projection of the endpoint of the NRM vector during AF demagnetization. Closed and open symbols represent end points of magnetization projected onto horizontal (N-S-E-W) and vertical (Up-Down-E-W) planes, respectively, in core coordinates. Peak fields and temperatures for selected AF steps and thermal demagnetization steps are shown. Depths in the cores are shown near sample names. (a, b, d, f, i) AF demagnetization only. (c, e) Thermal demagnetization after 10 mT AF cleaning. (g, h) Thermal demagnetization only. Light (dark) gray arrows correspond to the low (high) coercivity or low (high) temperature components.

755 and a Bartington MS2 susceptibility coil housed in the magnetically shielded laboratory (dc field <150 nT) in the Massachusetts Institute of Technology (MIT) Paleomagnetism Laboratory (web.mit.edu/paleomag). NRM components were determined using principal component analysis [Kirschvink, 1980] and Fisher statistics [Fisher, 1953] using the PaleoMac program [Cogné, 2003]. A set of 276 representative samples was demagnetized thermally or by three axis alternating field (AF) methods (Figures 3–6). To examine the effect of mixed AF and thermal demagnetization, we also thermally demagnetized dozens of pairs of sister samples taken ~ 1 cm apart, one of which had previously been subjected to AF demagnetization to 10 mT peak field (Figure 3). To obtain approximate (order of magnitude) paleointensity estimates, samples were given a laboratory thermoremanent magnetization (TRM) by cooling from 585°C (above the Curie temperature of magnetite) in a $50 \mu\text{T}$ field after completion of NRM demagnetization.

[18] Following AF demagnetization, 7 samples from VRED2 and 22 samples from VRED3 were given an anhysteretic remanent magnetization (ARM) in a peak ac field of 200 mT and a 2 mT dc bias field that was then stepwise AF demagnetized. This procedure was used to define the median demagnetizing field (MDF), the AF field at which half of the imparted ARM is demagnetized. Following this, the samples were given a stepwise IRM up to a field of 900 mT that was also then stepwise AF demagnetized. The IRM acquisition and AF demagnetization of IRM data are indicators of the coercivity spectrum of the sample and permit estimation of the remanent coercivity (H_{cr}).

[19] After completion of rock magnetic experiments, 5 samples from VRED2 and 15 from VRED3 were exposed to a saturating (2.5 T) field at 10 K after cooling in a zero field environment to measure their Verwey transitions. The moments of the samples were continuously measured every 5 K during heating in a zero field using a Quantum Design, Magnetic Property Measurement System (MPMS)

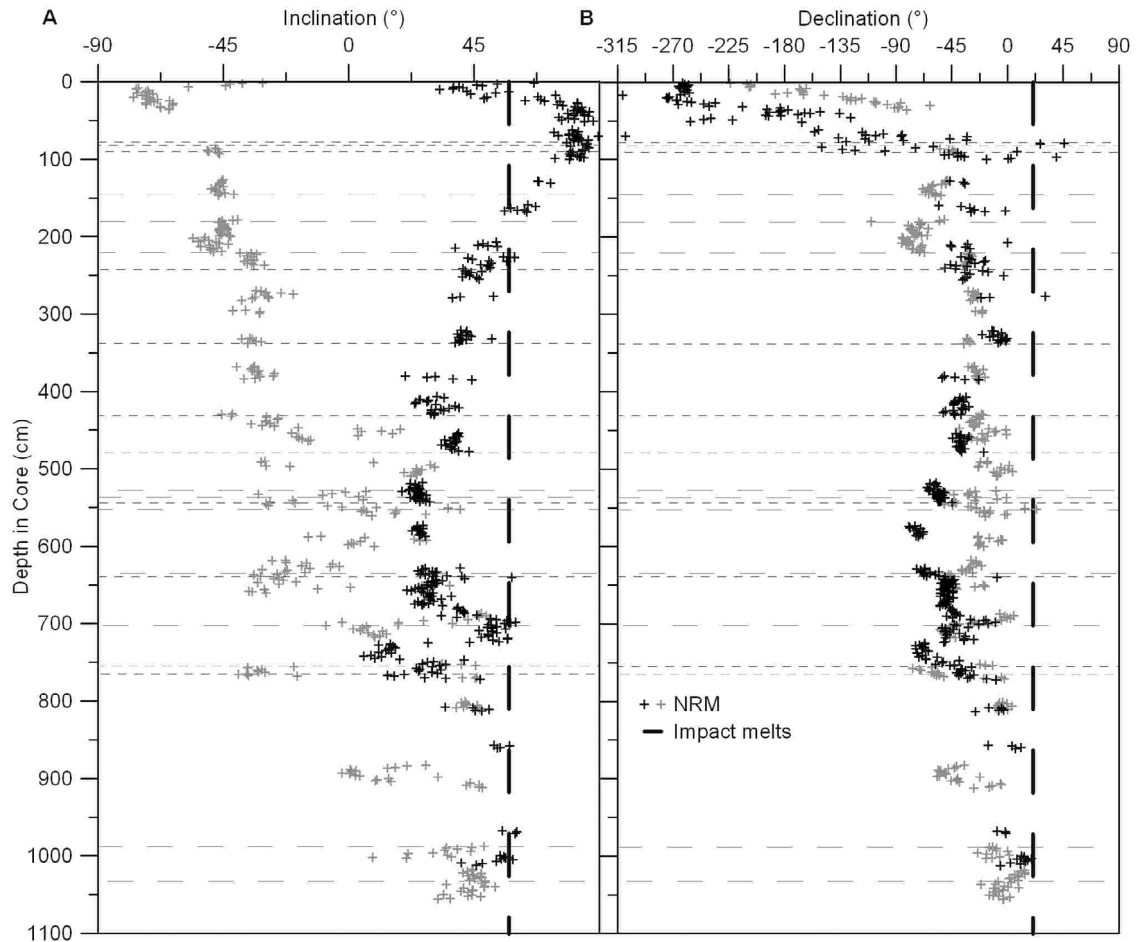


Figure 4. NRM directions from VRED2 (dark) and VRED3 (gray) cores. (a) Inclination. (b) Declination. Vertical dashed lines represent the mean direction of melt rocks around Vredefort crater measured by Carporzen *et al.* [2005]. Horizontal dashed lines represent breaks between core segments.

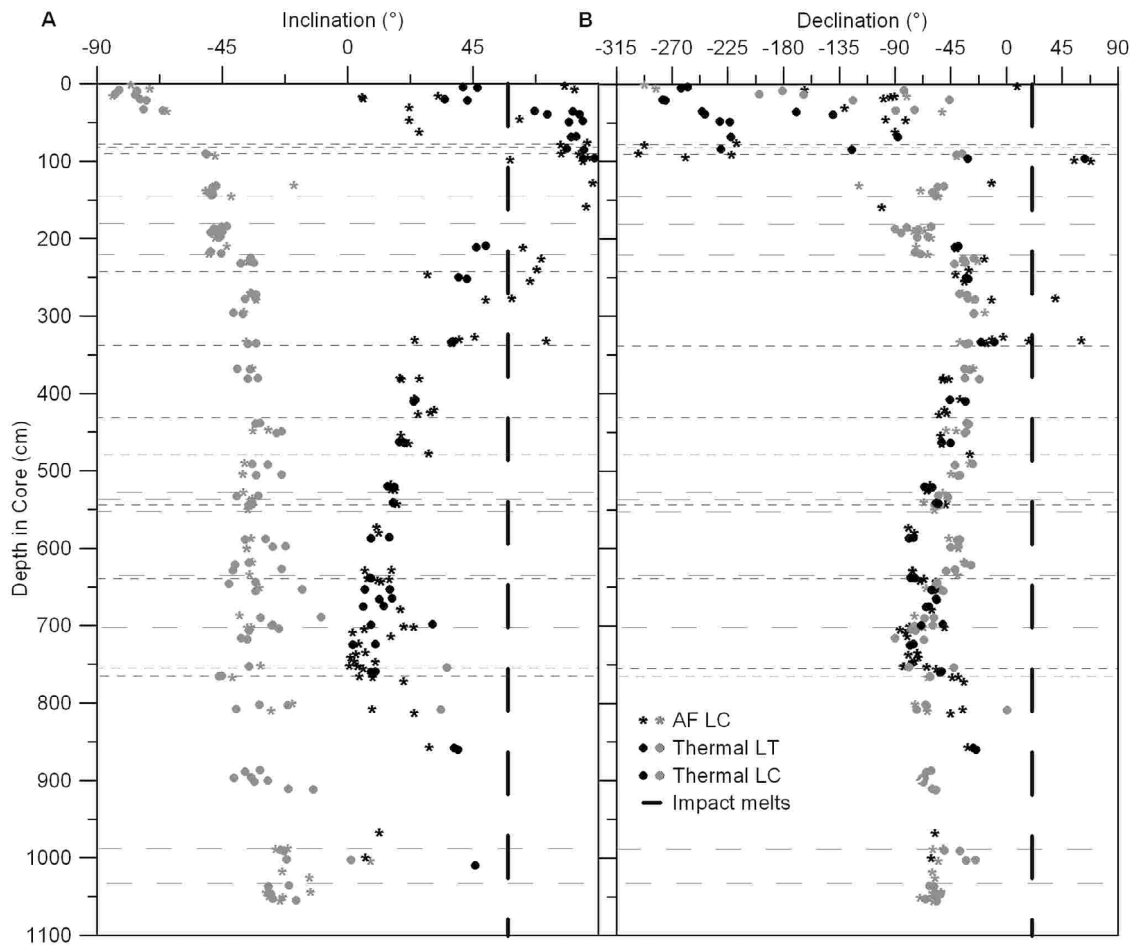


Figure 5. Low-coercivity (LC) and low-temperature (LT) overprint components isolated by AF (stars) or thermal demagnetization (dots for pairs of sister samples taken ~ 1 cm apart, one of which had previously been subjected to AF demagnetization to 10 mT peak field) from the VRED2 (dark) and VRED3 (gray) cores. (a) Inclination. (b) Declination. Vertical dashed lines represent the mean direction of melt rocks around Vredefort crater measured by *Carporzen et al.* [2005]. Horizontal dashed lines represent breaks between core segments.

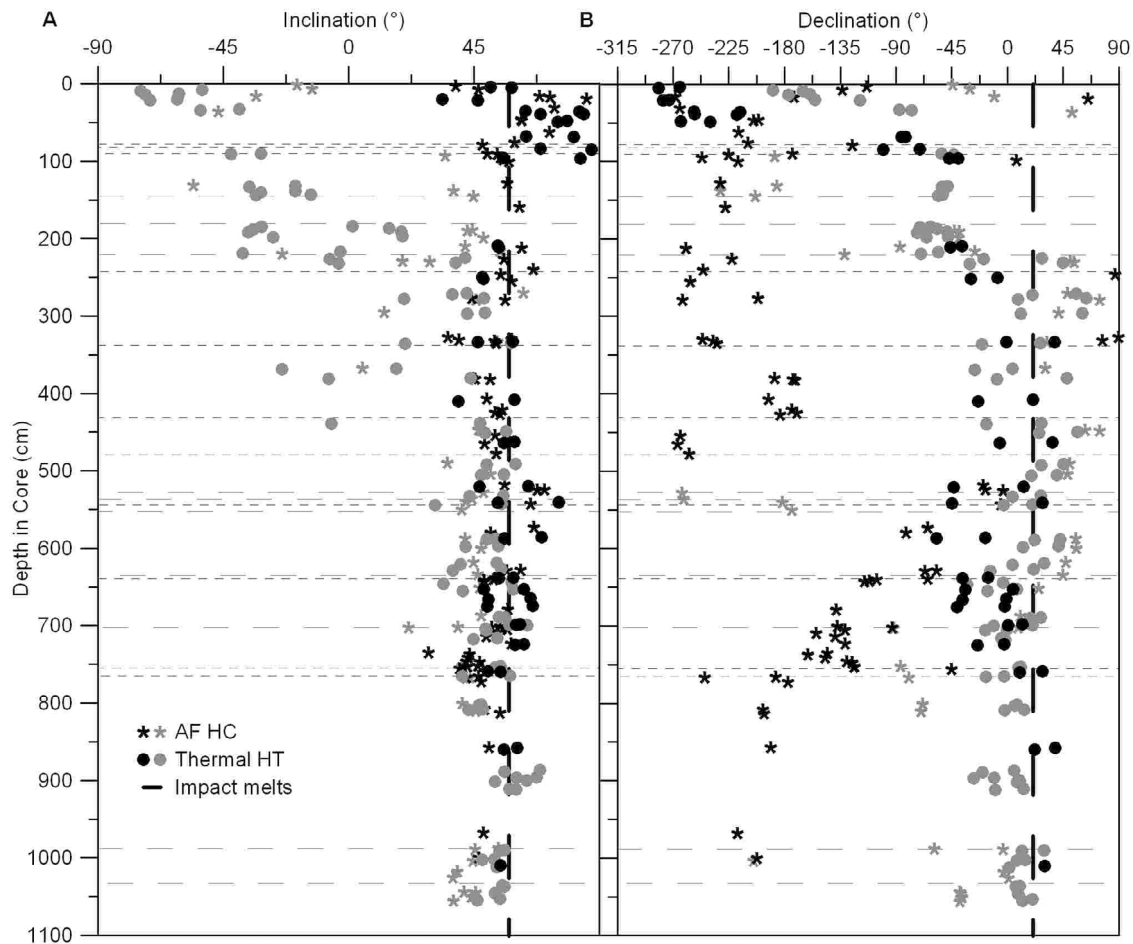


Figure 6. High-coercivity (HC) and high-temperature (HT) primary components isolated by AF (stars) or thermal demagnetization (dots) from the VRED2 (dark) and VRED3 (gray) cores. (a) Inclination. (b) Declination. Vertical dashed lines represent the mean direction of melt rocks around Vredefort crater measured by *Carporzen et al.* [2005]. Horizontal dashed lines represent breaks between core segments.

magnetometer in the Institut de Physique du Globe de Paris (IPGP) Paleomagnetism Laboratory.

3. Results

3.1. Geomagnetic Surveys and Surface Paleomagnetic Measurements

[20] The amplitude of the total field variations decrease from a peak value of $\sim 60,000$ nT at 55 cm height to $\sim 22,000$ nT at 2.55 m, at which point the field intensity and orientation are consistent with the IGRF model (Figure 2a). The geomagnetic anomaly vectors are collectively distributed along a common great circle (pole at $D_g = 37.1^\circ$, $I_g = 11.0^\circ$, $N = 494$, $\alpha_{95} = 37.4^\circ$; see Table 1 and Figure 2c) whose axis is oriented nearly horizontal and trending northeast-southwest. This axis, over ~ 30 m long, sharply separates positive and negative geomagnetic anomalies which laterally extend over 5 to 10 m (Figure 2b).

[21] The NRM intensities of the 100 surface samples range from 0.2 and 450 A/m with a mean of 34.7 A/m and a median of 15.5 A/m, while susceptibilities are spread over more than four orders of magnitude with Q ratios above 10. The NRM directions fall on a swath that roughly defines a great circle

(pole at $D_g = 219.2^\circ$, $I_g = 5.8^\circ$, $N = 100$, $\alpha_{95} = 40.0^\circ$; see Table 1 and Figure 2c) whose axis is closely associated with the anomaly field directions at 55 cm height. This coherence demonstrates that these rocks are the source of the large-scale field anomalies, while the scatter in the NRM directions off the overall great circle pattern indicates that there is also a fine-scale (< 55 cm) random magnetization pattern superposed on the surface.

3.2. Reconstruction of the Orientation in the Semicontinuous Cores

[22] The vertical orientation is known along the full 10 m length of each core. Thus, the NRM inclination in core coordinates (I_c) can be absolutely compared between samples from within each core (Table 2). We found that the shallow parts ($\sim < 5$ m) of the cores have NRM inclinations I_c opposite in sign (Figures 3 and 4). Given that the VRED2 and VRED3 cores have hade within 13° of vertical and azimuths in the same direction of ~ 210 – 215° , this indicates that the cores have absolute NRM inclinations (I_g) opposite in sign, consistent with the field anomalies measured 0.55 m above the surface (see section 3.1). The NRM inclinations in both boreholes change rapidly within the first meter and ultimately

Table 1. Fisher Statistical Analysis [Fisher, 1953] for Geomagnetic Anomaly Vectors and for Standard Paleomagnetic Samples in Geographic Coordinates^a

Name	D_g (°)	I_g (°)	N	k	α_{95} (°)
<i>Geomagnetism</i>					
0.55 m survey mean direction	310.9	26.7	100	2.3	12.5
0.55 m survey great circle pole	51.0	16.0	100	GC	36.4
1.20 m survey mean direction	128.4	-2.6	196	5.8	4.6
1.20 m survey great circle pole	215.0	-2.1	196	GC	42.8
2.55 m survey mean direction	125.8	-1.1	196	15.3	2.7
2.55 m survey great circle pole	215.7	-7.3	196	GC	38.9
<i>Surface Samples</i>					
NRM of the 100 square grid samples	302.2	-52.9	100	2.7	10.7
HC/HT basements rocks from surface outcrops	8.5	67.5	319	2.4	6.6
HC/HT pseudotachylites and basement rocks from quarries	13.7	58.6	110	10.8	4.3
HC/HT pseudotachylites and basement rocks from surface outcrops	4.5	67.2	93	2.8	11.0
HC/HT selected pseudotachylites and basement rocks	15.4	56.7	119	56.3	1.7

^aThe first column gives the average name, the second column gives the mean component declination, the third column gives the mean component inclination, the fourth column gives the number of average directions, the fifth column gives the precision parameter, and the sixth column gives the 95% confidence interval. NRM, natural remanent magnetizations; HC, high coercivity; HT, high temperature; GC, great circle (indicates a least squares plane fit).

reach similar positive inclinations below 10 m depth (core inclination $I_c = 40.0^\circ$ in VRED2 and $I_c = 33.0^\circ$ in VRED3 (Table 2)). While the angular difference between the orientations of the two cores is only 7.2° (2° between the two hades and 7.1° between the two azimuths), conversion from core coordinates (I_c and declination D_c) to geographic coordinates (I_g and D_g) should be relatively similar for each core. Because both I_g and D_g depend on the unknown magnetization declination in core coordinates, D_c , the magnetization orientation in geographic coordinates cannot be determined from I_c only (see Appendix A). Furthermore, there is no trace of a present-day field viscous remanent magnetization that could be used to orient the cores at depth. However, the last sample of the first 0.8 m section of VRED2 core and the two last samples of the first 1.45 m section of VRED3 core, which are absolutely oriented in both declination and inclination, have high-coercivity (HC) components ($D_g = 343.0^\circ$, $I_g = 69.8^\circ$ at 0.76 m in VRED2 and $D_g = 336.5^\circ$, $I_g = 43.7^\circ$ at 1.38 m and $D_g = 6.7^\circ$, $I_g = 54.5^\circ$ at 1.45 m in VRED3, see section 3.3) within only ~ 10 to 30° of the impact melt mean directions [Carpornzen et al., 2005; Salminen et al., 2009]. Therefore, we assumed that the magnetization at greater depths should be uniform in both cores in both absolute inclination and declination and in the vicinity of the impact melt mean directions. To recover from the 11 and 10 unknown rotations between core segments in VRED2 and VRED3, respectively, we rotated each lower section until the geographic declination D_g of the vector sum of the HC components (see section 3.3) over each segment is $\sim 25^\circ$, omitting a few outliers with incoherent directions. We estimate that this correction leads to an uncertainty of at least 5° in the rotated segments. Henceforth, we discuss the magnetization directions in absolute (geographic) coordinates (D_g and I_g).

3.3. Paleomagnetism of the 10 m Drill Cores

[23] The NRM directions in both boreholes lie along a nearly vertical great circle (strike $\sim 139^\circ$ and dip $\sim 79^\circ$), calculated using a least squares plane fit to the NRM directions of all 722 samples (Figure 7a). Our AF and thermal demagnetization of selected subsamples isolated low coercivity (LC) components that usually unblock by 10 mT (Figure 3) and low temperature (LT) components typically unblock by either between 100°C and 400°C (for the bottom half of each core) and sometimes up to 530°C (in the top half of each core). After removing these components, we isolated a high-temperature (HT) component between 550°C and 585°C and a high-coercivity (HC) component from 10 to 40 mT up to the last AF demagnetization step (85 or 290 mT). Both the HT and HC components trend linearly toward the origin upon progressive stepwise demagnetization.

[24] Below several meters depth, both the inclination and declination of the HT and HC components cluster within each core as well as between the two cores (Figures 6 and 7c). Below 1 m depth, the LC and LT overprints are relatively well clustered within each core and have declinations pointing toward the northwest but have very different mean inclinations (Table 2, Figures 5 and 7b). The HC and HT directions are scattered in the upper parts of the cores, but become well clustered at depths greater than 1–3 and 5–7 m, in VRED2 and VRED3, respectively. Below ~ 10 m, the HC/HT components are essentially the same as the NRM directions prior to demagnetization (Figures 4 and 7a). The mean HC and HT component inclinations I_g

Table 2. Maximum Likelihood Fisher Statistical Estimate of the Mean Inclination [Cogné, 2003; McFadden and Reid, 1982] in Core Coordinates I_c and Fisher Statistical Analysis [Fisher, 1953] for Both Alternating Field and Thermal Demagnetization on Samples From the Two 10 m Deep Cores^a

Name	N	I_c (°)	\pm (°)	D_g (°)	I_g (°)	k	α_{95} (°)
<i>VRED2 Core</i>							
NRM below 10 m	10	40.0	4.6	9.6	52.6	117.9	4.5
LC	96	27.6	6.2	313.3	33.3	6.7	6.0
LT	30	35.9	15.2	307.7	34.9	3.1	18.0
HC	76	53.3	2.7	17.0	69.8	17.6	4.0
HT	50	51.1	4.5	359.9	68.5	11.0	6.4
HC below 1 m	61	51.7	2.5	18.1	67.1	23.4	3.8
HC below 7.5 m	12	46.5	2.9	19.6	60.8	36.7	7.3
HT below 6.9 m	10	45.1	4.1	12.4	58.4	57.3	6.4
<i>VRED3 Core</i>							
NRM below 10 m	33	33.0	3.4	358.4	42.3	51.6	3.5
LC	100	36.3	3.6	283.2	-38.9	12.1	4.2
LT	50	37.0	4.3	286.0	-38.7	9.1	7.1
HC	50	40.4	4.1	21.0	54.0	13.4	5.7
HT	100	36.7	3.3	16.3	54.1	4.9	7.1
HC below 3 m	31	42.3	4.1	21.3	53.5	43.2	4.0
HC below 8 m	11	43.2	3.7	18.6	53.8	206.1	3.2
HT below 5 m	52	42.3	2.5	6.7	53.0	40.3	3.1
HT below 9 m	13	43.6	2.8	11.0	53.9	173.5	3.2

^aThe first column gives the average name, the second column gives the number of average directions, the third column gives the Fisher estimate of the mean inclination in core coordinates, the fourth column gives the confidence interval, the fifth column gives the mean component declination in geographic coordinates, the sixth column gives the mean component inclination in geographic coordinates, the seventh column gives the precision parameter, and the eighth column gives the 95% confidence interval. LC, low coercivity; LT, low temperature.

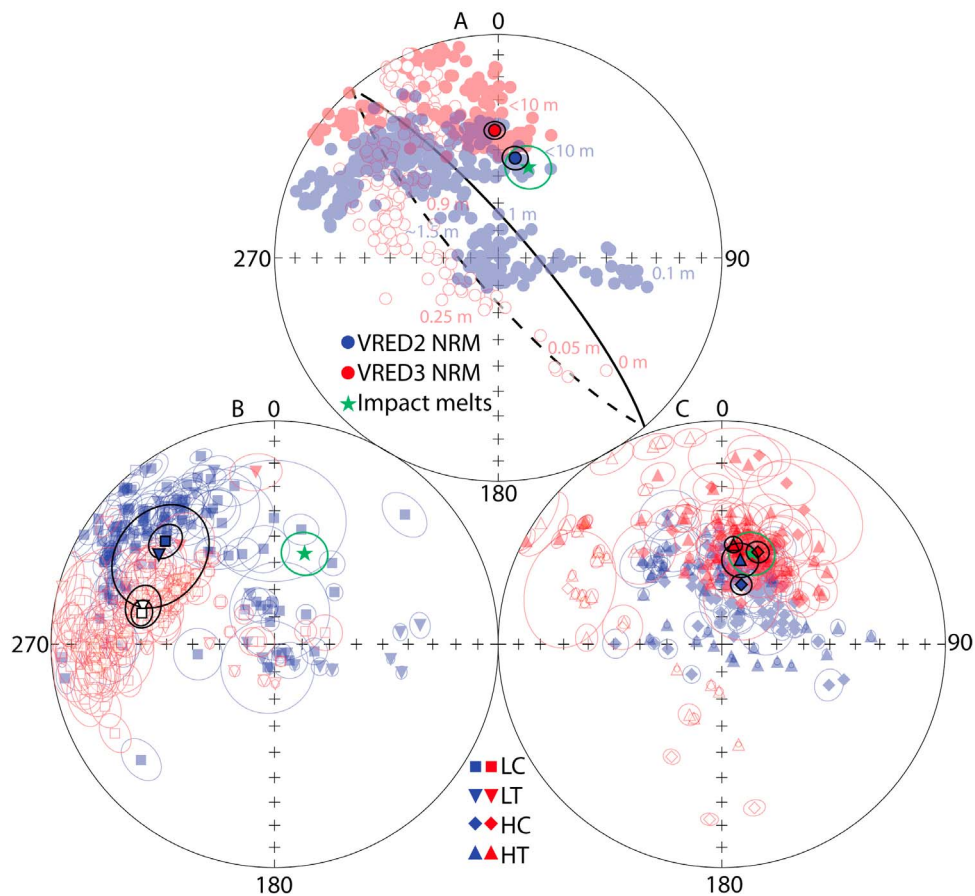


Figure 7. Equal area stereonets showing NRM directions isolated from VRED2 (blue) and VRED3 (red) cores. (a) NRM (circles). (b) Low-coercivity (LC) (squares) and low-temperature (LT) (inverted triangles) magnetization components. (c) High-coercivity (HC) (diamonds) and high-temperature (HT) (upright triangles) magnetization components. Depths of selected samples are shown in Figure 7a. Uncertainty ellipsoids are defined as maximum angular deviations associated with the least squares fits. Solid symbols and corresponding ellipsoids represent average directions and associated 95% confidence intervals (see Table 2). Great circle shown in Figure 7a is the least squares fit to the 722 NRM directions from the two cores. Green stars and associated ellipsoids (95% confidence intervals) represent the average impact melt direction obtained by *Salminen et al.* [2009] which is indistinguishable at 95% confidence limits from the average impact melt direction of *Carporzen et al.* [2005]. Solid symbols correspond to lower hemisphere; open symbols and dashed lines correspond to upper hemisphere.

at depth (below $\sim 7\text{--}8$ m) are 60.8° and 58.4° and 53.8° and 53.9° for VRED2 and VRED3, respectively (Table 2). These inclinations are indistinguishable from the $\sim 55\text{--}57^\circ$ paleomagnetic inclination of the Vredefort impact melt rocks [*Carporzen et al.*, 2005; *Salminen et al.*, 2009].

[25] Both the magnetic anomaly vectors measured 0.55 m above the surface and the NRM directions of the top few meters of the 10 m cores lie mostly along a common vertical great circle (Figures 2c and 7a). These magnetization patterns and geomagnetic anomalies are consistent with the circular field expected from a current flowing horizontal and in the northeast direction. This magnetization pattern is very similar to other observations of drill core samples from lightning remagnetized rocks [e.g., *Graham*, 1961, Figures 9 and 10].

[26] Near-surface samples from the boreholes have high NRM intensities and high Q ratios similar to those observed in outcrops around Vredefort [*Carporzen et al.*, 2005;

Salminen et al., 2009], yet both quantities decrease rapidly with depth in each borehole (Figure 8). Paleointensity estimates (ratio of NRM to a $50\ \mu\text{T}$ laboratory TRM on 150 samples) follow similar trends with depth, decreasing from $\sim 600\ \mu\text{T}$ at the surface to $\sim 37\ \mu\text{T}$ at ~ 2 m depth. The latter value is in general agreement with the paleointensity of the Earth's magnetic field at ~ 2 Ga (Figure 8) [*Macouin et al.*, 2004]. REM (NRM/IRM(0.9 T)) [*Kletetschka et al.*, 2004] and the mean of the derivative of this ratio through AF demagnetization between 35 and 85 mT (REM' [see *Gattacceca and Rochette*, 2004]) both show the extreme efficiency of the NRM near the surface with ratios close to 1, that decrease rapidly with depth (Figures 8 and 9).

[27] The rock magnetic properties of the core samples also change rapidly with depth. The samples with the greatest H_{cr} and MDF values are found near the surface, where they range up to 44 and 31.7 mT, respectively (Figure 10a). Below

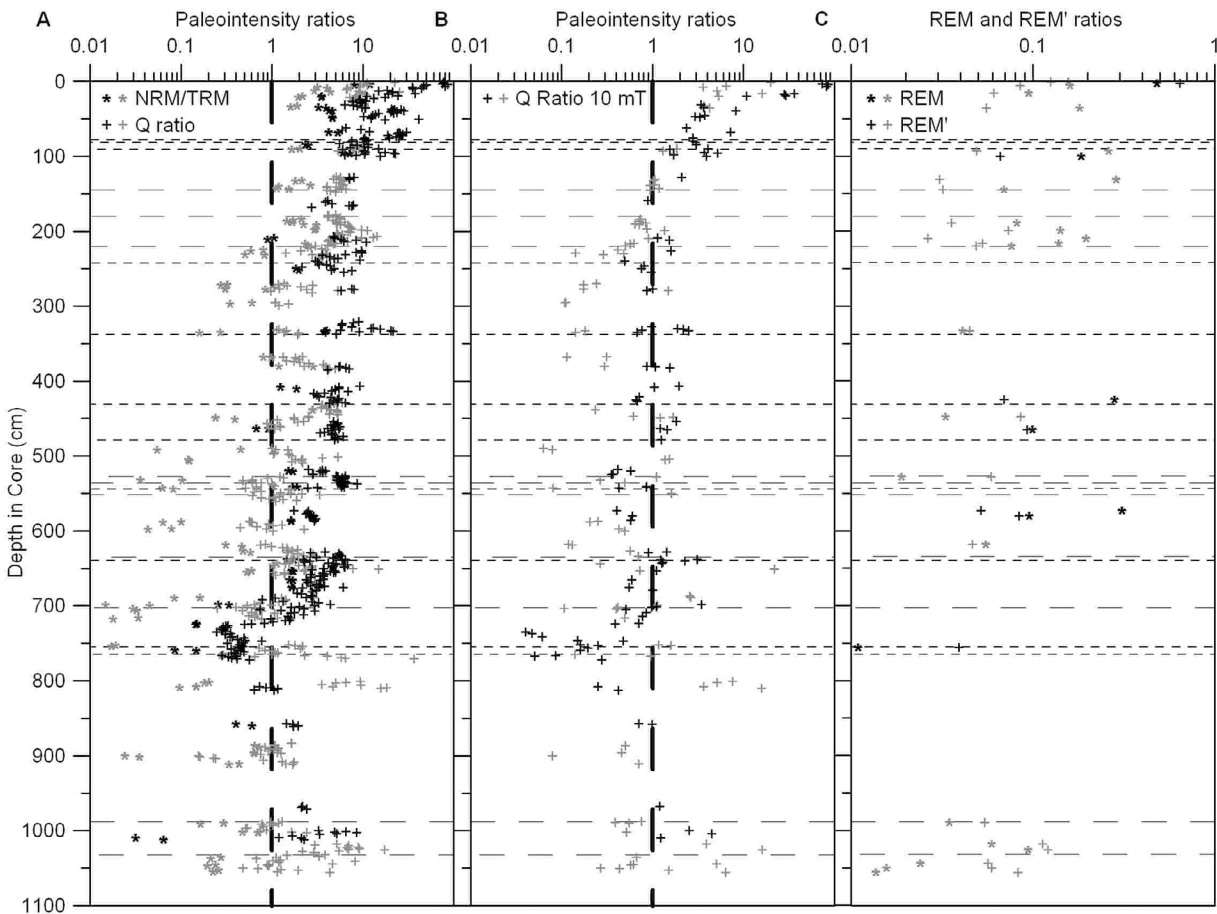


Figure 8. Summary of paleointensity experiments for the VRED2 (dark) and VRED3 (gray) cores. (a) Semilog plot showing paleointensity ratios defined as the ratio of NRM to a $50 \mu\text{T}$ laboratory thermoremanent magnetization (TRM) (stars) and the Koenigsberger Q ratio (crosses). (b) Semilog plot showing the Koenigsberger Q ratio 10 mT (crosses) using the moment after the 10 mT AF step. Vertical dashed line at 1 represents a paleointensity of $50 \mu\text{T}$ for TRM ratios and $30 \mu\text{T}$ for Q ratios. (c) Semilog plot of the remanent magnetization (REM) and REM' ratios defined as the NRM over the laboratory isothermal remanent magnetization (IRM) (stars) and the mean of its derivative computed between 35 and 85 mT (crosses) [Gattacceca and Rochette, 2004; Kletetschka et al., 2004]. Horizontal dashed lines represent breaks between core segments.

36 cm depth, H_{cr} and MDF decrease to 13.5 ± 1.9 mT (1σ) and 8.5 ± 1.3 mT (1σ), respectively. In samples from all depths, we identified a Verwey transition in the vicinity of 120–130 K (determined as the maximum of the derivatives of the moment-temperature data with respect to temperature). This Verwey transition (HT-Tv in the work of Carporzen et al. [2006]) was the only transition identified at depths below 36 cm (Figures 9a and 10b). Importantly, we found in all 5 samples from above 36 cm depth a second Verwey transition occurring at temperatures between 90 K and 110 K (Figures 9a and 10b). This is absent from all samples below this depth. As discussed in section 1, this second low-temperature Verwey transition (LT-Tv) was previously identified in magnetic fractions smaller than $15 \mu\text{m}$ in 29 surface Vredefort basement rocks from localities throughout the crater [Carporzen et al., 2006], and was interpreted to be related to impact-generated, PDF-hosted SD

and/or PSD magnetite following Cloete et al. [1999], Hart et al. [2000] and Nakamura et al. [2010]. In summary, the magnetic mineralogy near the surface is characterized by relatively high coercivity and by the presence of two Verwey transitions characteristic of a mixture of Archean MD and smaller ($<15 \mu\text{m}$) magnetite grains. The high-coercivity and double-Verwey transitions are not present at depth below ~ 36 cm.

3.4. Analysis of Surface Samples From Around Vredefort

[28] AF and thermal demagnetization were performed on additional surface samples from around the Vredefort crater. These augment by a factor of 3 the original suite of basement rocks and pseudotachylites analyzed by Carporzen et al. [2005] by incorporating new samples from their same sites and additional samples from 21 new localities (Figure 1). Our new, enlarged data set confirms the observation by

Carporgen *et al.* [2005] and Salminen *et al.* [2009] that HC and HT components in granitoid rocks sampled in surface outcrops are overall statistically random (Figure 11a), with less than 10 samples out of 319 in the vicinity of the impact melt direction. However, our new data set also demonstrates that the subset of pseudotachylite and surrounding granitoid

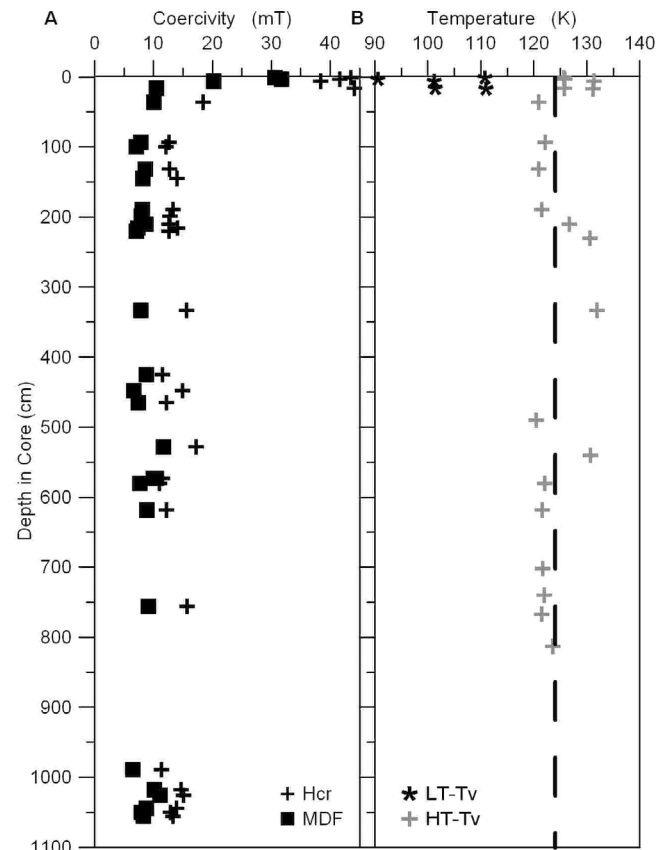
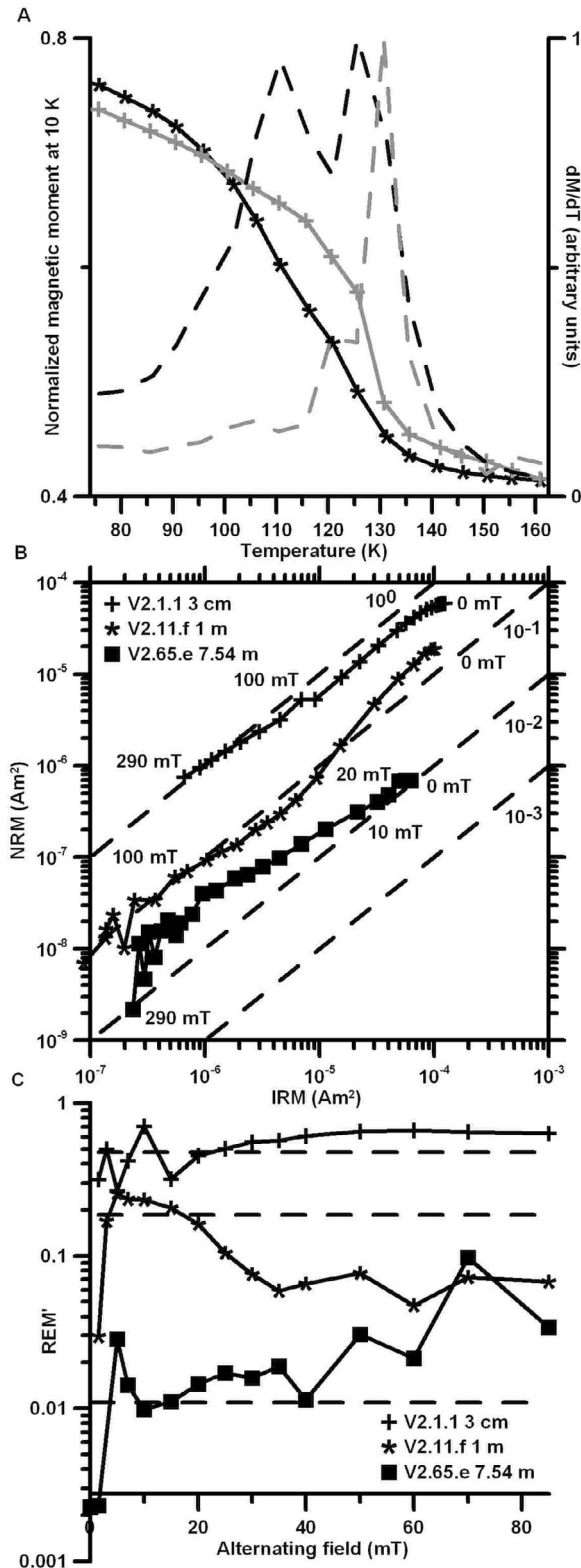


Figure 10. Summary of rock magnetic experiments for both 10 m deep cores. (a) Remanent coercivity (H_{cr} , crosses) and median demagnetizing field (MDF, squares) of ARM (acquired at 200 mT AC field with a 2 mT DC field). (b) High- and low-temperature Verwey transitions (HT-Tv and LT-Tv), defined as the extrema of the derivative of the moment-temperature data with respect to the temperature. Vertical dashed line at 124 K represents the temperature of the Verwey transition for pure stoichiometric magnetite.

samples that were taken from quarry walls or recently excavated surfaces in quarries have much more clustered HC and HT components (119 samples out of 204) (Table 1 and Figure 11b). In particular, 41 of the 66 granitoid samples

Figure 9. (a) Representative thermal demagnetization of a 10 K saturation IRM and normalized (to maximum value at 10 K) derivative curves for samples V3.1.e (1 cm deep, black) and V3.45.e (540 cm deep, gray) from the VRED3 core. The latter sample is characterized by a unique high-temperature Verwey transition at ~ 130 K whereas the former sample has two Verwey transitions at temperatures of ~ 125 K and ~ 110 K. (b) Evolution of NRM and IRM during AF demagnetization for samples at three different depths from the VRED2 core. Peak fields for selected steps are shown. Dashed lines are isovalues of remanent magnetization (REM) ratios = NRM/IRM . (c) REM' ratio versus alternating field for the same samples shown in Figure 9b. Total REM ratios are indicated by the dashed lines. REM' ratios shown in Figure 8c are the mean value from 40 to 85 mT.

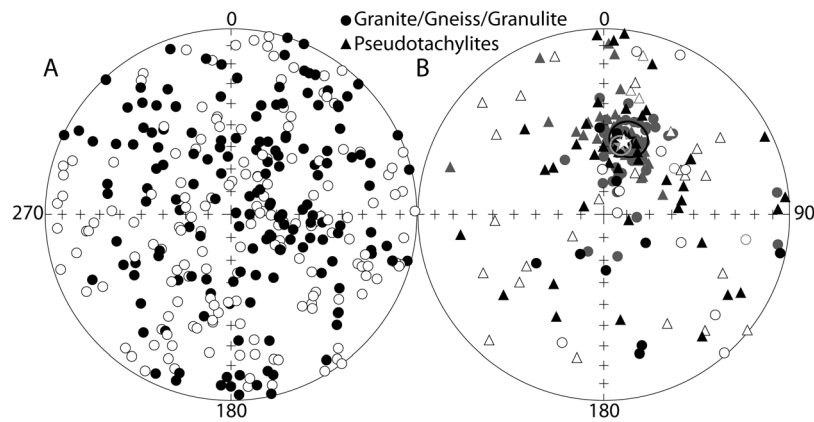


Figure 11. (a) Equal area stereonet showing high-coercivity (HC) and high-temperature (HT) magnetization components determined for 319 samples collected at 110 sites of basement rocks exposed on erosion surfaces. (b) Equal area stereonet showing HC and HT components determined for 204 samples of pseudotachylites and surrounding basement rocks taken from 26 sites. Of these 26 sites, 13 sites were located in quarries (gray symbols) and 13 were located at natural erosion surfaces (black symbols). Grey star and associated ellipsoid represent the averaged direction and associated 95% confidence intervals for samples from quarries (Table 1). White star (95% confidence ellipsoid smaller than the star itself) represents the average direction for selected samples from both erosion surfaces and quarries (Table 1). Black star and associated 95% confidence ellipsoid represent the impact melt average direction obtained by *Salminen et al.* [2009]. Solid symbols correspond to lower hemisphere; open symbols and dashed lines correspond to upper hemisphere.

from quarry walls or excavated surface have the same magnetization directions as that recorded in surrounding pseudotachylites.

3.5. Electrical Conductivity and Implications for Susceptibility to LIRM

[29] We have shown that unlike the granitoid samples, melt rocks tend to have more clustered NRM directions that are close to that expected for the 2 Ga pole position for South Africa. In two instances, we collected granite/granulite rocks within a few meters of the dykes, yet the dykes show little evidence for an LIRM whereas the granite/granulite facies do (although this difference is not observed in quarries; see below). Hysteresis parameters of both are similar so differences in the relative abundance of SD versus MD grains can be ruled out.

[30] One possibility is that the granites are more susceptible to LIRM because they stand higher or are less protected by vegetation. Within the ring around the Vredefort basement rocks formed by the Witwatersrand quartzites, the topography is relatively flat. Our field observations show that basement rocks and pseudotachylites are eroded with about the same rate (with the latter, if anything, slightly more resistant), whereas granophyre dykes are more resistant, forming slight topographic highs. Tree coverage is sparse, mostly confined along the Vaal River or near roads and farms. No particular lithology seems to enhance tree growth that would potentially protect outcrops from lightning.

[31] Another possibility is that the dykes avoided remagnetization because they have lower conductivity than the granitoids, which shielded them from currents flowing in the ground. To test this possibility, we measured the electrical

conductivity of both dyke and granitoid lithologies. The goal was to determine whether the dyke lithologies have lower conductivity, which might shield them from lightning-induced currents in the ground. Electrical impedance measurements were performed at MIT using a Solartron 1260 impedance spectrometer at room pressure and temperature on dry cylindrical rock samples (height = 2 to 13 mm, diameter = 6 or 25 mm). These were taken from four surface granules and six granules from the two 10 m deep cores as well as outcrops of one granophyre dyke and two pseudotachylites. We used a two electrodes setup in which carbon was evaporated as electrodes on both sides of the cylinders (carbon thickness $\sim 0.4 \mu\text{m}$) [*Malki and Echegut, 2003*]. The complex electrical impedance was measured over a wide frequency domain (1 MHz to 10 Hz) [*Huebner and Dillenburg, 1995*]. The conductivity was calculated using $\sigma = G/R$ where σ is the electrical conductivity (S/m), R is the electrical resistance (ohm) (determined from the real part of the complex impedance) and G is a geometric factor (cylinder length/coated disk surface) (m^{-1}).

[32] We found that samples from the two 10 m deep cores have conductivities of the same order of magnitude, regardless of lithology ($\sigma = 10^{-6.13 \pm 0.15}$ S/m ($N = 6$) for the cores samples, $\sigma = 10^{-5.28 \pm 0.12}$ S/m ($N = 7$) for standard surface samples and $\sigma = 10^{-5.67 \pm 0.46}$ S/m ($N = 13$) for all samples). This demonstrates the negligible effects of lithology on the electrical properties of the investigated samples. Therefore, our electrical conductivity measurements suggest that no lithology should be preferentially susceptible to being remagnetized by lightning currents traveling through the ground. In summary, it is not completely clear why the melt rocks

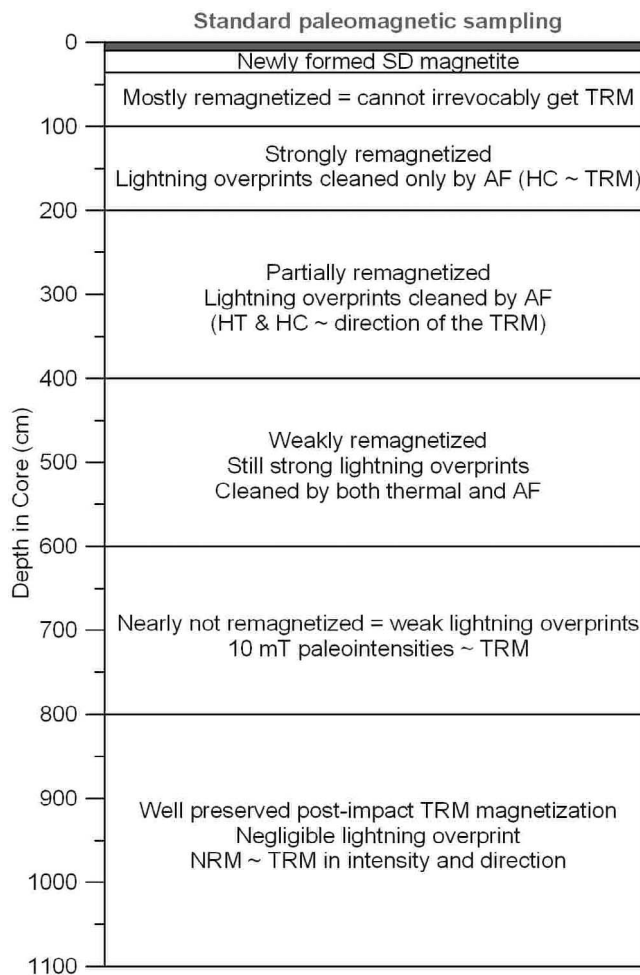


Figure 12. Summary of the effects of lightning on rock magnetic and paleomagnetic data as a function of depth in the VRED2 and VRED3 cores.

exposed in surface outcrops seemed to be less affected by LIRM than granitoid rocks.

4. Discussion

[33] Our paleomagnetic study of the two ~ 10 m drill cores clearly shows that the random magnetization directions and high magnetization efficiencies are near-surface features of the Vredefort basement rocks (Figure 12). Deeper samples preserve the magnetization previously observed in some impact melt rocks [Carporzen *et al.*, 2005; Hargraves, 1970; Jackson, 1982; Salminen *et al.*, 2009] (Figures 10 and 11), suggesting that the basement rocks near the center of Vredefort cooled through the 580°C magnetite Curie temperature after impact and tectonic readjustments, as suggested by Henkel and Reimold [1998, 2002], Jackson [1982], Muundjua *et al.* [2007] and Salminen *et al.* [2009].

[34] The vertical and horizontal spatial distribution of the magnetization directions, together with the geomagnetic surveys at three altitudes, are consistent with the simple geometry of a horizontal, semicylindrical magnetization pattern with magnetic field lines reconnecting at the missing top of the cylinder (Figure 2 and Figures 4–8, similar to

Figures 9–12 and 16 of Graham [1961] and Figure 10 of Shimizu *et al.* [2007]). This geometry suggests that a horizontal lightning current oriented northeast-southwest flowed between the two borehole locations and remagnetized the outcrop extending for over 40 m [Graham, 1961; Shimizu *et al.*, 2007]. LC component directions are neither parallel to the expected present-day geomagnetic field nor oriented along the axis of the cores, ruling out their origin as a viscous remanent magnetization or as a drilling-induced overprint, respectively. Thus, we conclude the LC and LT overprints both in the 10 m deep cores and in the plethora of surface samples owe their origin to lightning. For samples from below ~ 1 m depth, AF demagnetization removes this LIRM (Figure 8) to reveal the postimpact thermoremanence, which has a characteristic low magnetization efficiency (for NRM blocked above AF 10 mT, median $Q = 0.71$ and median $REM' = 0.0565$). The effects of lightning on rock magnetic and paleomagnetic data as a function of depth are summarized in Figure 12.

[35] Our study further suggests that magnetite grains that have high coercivities and are responsible for the LT Verwey transitions observed throughout Vredefort surface samples [Carporzen *et al.*, 2006] were not produced by the impact but have a much more recent origin. We believe these grains were produced as a result of lightning-induced melting, although a weathering origin cannot entirely be excluded. Even though a weathering origin is consistent with the increase in coercivity observed in surface samples [van Velzen and Zijdeveld, 1995], we consider this explanation unlikely. First, our thermal demagnetization experiments show no evidence for any minerals near the surface except for magnetite (no evidence for the 680°C Curie point of hematite, the 150°C Curie point of goethite, or the inversion of maghemite to hematite [Dunlop and Ozdemir, 1997]). Second, oxidized magnetite will have a softer (or even lack) Verwey transition at lower temperature that becomes progressively more poorly defined [Ozdemir *et al.*, 1993]. Although the LT-T_v of the surface samples does indeed have a lower temperature than the HT-T_v of deeper samples, it still exhibits a fairly sharp drop with temperature. Finally, as discussed above, we found no evidence of a present-day field overprint that could have resulted from recent weathering. Thus, it appears that the most likely origin for much of the high-coercivity magnetite is lightning, which is also known to produce melts ranging from micrometer-scale melt pockets to meter-sized fulgurites [Appel *et al.*, 2006; Carter *et al.*, 2010; Essene and Fisher, 1986; Frenzel *et al.*, 1989; Jones *et al.*, 2005]. The presence of glassy material within the planar deformation features suggests very rapid ($< 1 \mu\text{sec}$) cooling times of the newly created phases. Such quickly cooled melts are likely to contain fine-grained magnetite that should preferentially form SD-sized grains, which have high coercivity relative to MD grains.

[36] Because the near-surface magnetite has a higher coercivity than the Archean multidomain magnetite, it is more resistant to AF demagnetization and may efficiently mask any 2 Gyr old TRM record that may have survived remagnetization by lightning. However, our preliminary analysis of 20 thin sections take from rocks at varying depths throughout both cores showed that the amount of decorated PDFs appeared fairly constant with depth. Further petrographic studies are needed to characterize the variability

of magnetite that could be produced by lightning in the Vredefort rocks, PDF-hosted SD and/or PSD around biotite.

[37] Ground geomagnetic surveys of the Vredefort granites found numerous 10 m² sized patches with strong magnetic gradients [Muundjua *et al.*, 2007], indicating that our studied area is rather characteristic of Vredefort basement rocks (Figure 2). Given the frequency of lightning strikes in the Vredefort area as indicated either by satellite imagery (20 flashes/km²/yr, about two thirds of which strike ground) [Christian *et al.*, 2003] and by a lightning detection network (10–15 flashes/km²/year, 90% of which strike ground) [Gill, 2008], and assuming that about 10 m² are remagnetized by one lightning strike (see Figure 2b and the work of Muundjua *et al.* [2007]), we calculate that the entire Vredefort basement should be covered by lightning strikes over a period of 750 years. Previous studies of lightning remagnetization indicate that rocks are typically remagnetized below the surface down to depth of about the lateral radius of the cylindrical or polar geometry seen at surface [Appel *et al.*, 2006; Graham, 1961; Sakai *et al.*, 1998; Tauxe *et al.*, 2003; Verrier and Rochette, 2002]. Our cores show that at least partial LIRM can extend down to ~8 m depth (Figure 12), with the first meter being completely remagnetized (Figure 12). Given that erosion rates on the Kaapvaal craton are presently as low as 1 μm/yr [Burke and Gunnell, 2008], a lightning-remagnetized surface layer would be hardly affected by erosion for over 750 years. Thus, surface samples in Vredefort basement rocks should mostly be lightning remagnetized except for those from areas of localized high erosion or recently excavated locations like quarries. This explains why pseudotachylite and granitoid samples collected from quarries preferentially retain a 2 Ga thermoremanence. Because the pseudotachylite samples analyzed by Carporzen *et al.* [2005] were preferentially sampled in quarries, this also explains why they observed that pseudotachylites have clustered directions relative to granitoid samples which were sampled mostly outside of quarries.

5. Conclusion

[38] Petrographic observations of Vredefort granitoid rocks collected near the surface identified magnetite and other mineral phases within PDFs. This led to the interpretation that the PDF-hosted magnetite formed because of the impact event. Subsequent studies showed that the majority of surface granitoid rocks, many of which contain this newly formed magnetite, carry a magnetization characterized by randomly oriented directions and strong intensities. Our new observations from borehole data clearly show that previous conclusions drawn from surface samples, in particular the impact plasma-generated magnetic field, fluid circulation, and “super magnetic rocks” are incorrect. At Vredefort, lightning remagnetization rather than fluid circulation [Salminen *et al.*, 2009] almost certainly accounts for the high Koenigsberger Q ratios and intense and scattered magnetization direction of the surface samples at Vredefort [Carporzen *et al.*, 2005; Hart *et al.*, 1995; Hart *et al.*, 2000; Salminen *et al.*, 2009]. Furthermore, our study is consistent with the interpretation that nearly the whole Vredefort basement acquired a 2 Ga thermal overprint of the Earth’s magnetic field after tectonic readjustments following impact. This removes a key piece of evidence thought to support the

hypothesis that impacts can generate transient magnetic fields that will lead to substantial remagnetization of target rocks.

Appendix A: Dependency of the Magnetization Declination in Core Coordinates, D_c

[39] The core coordinate magnetization inclinations and declinations are obtained from the orthogonal magnetization components using:

$$\begin{cases} I_c = \tan^{-1} \left[\frac{Z_c}{\sqrt{X_c^2 + Y_c^2}} \right] \\ D_c = \tan^{-1} \left[\frac{Y_c}{X_c} \right] \end{cases} \Rightarrow \begin{cases} I_g = \tan^{-1} \left[\frac{Z_g}{\sqrt{X_g^2 + Y_g^2}} \right] \\ D_g = \tan^{-1} \left[\frac{Y_g}{X_g} \right] \end{cases} \quad (A1)$$

where X , Y , and Z are the three orthogonal components of the magnetization, with subscripts c and g referring to core and geographic coordinates, respectively:

$$\begin{cases} X_c = M \cos I_c \cos D_c \\ Y_c = M \cos I_c \sin D_c \\ Z_c = M \sin I_c \end{cases} \Rightarrow \begin{cases} X_g = X_c \cos H - Y_c \sin Az + Z_c \sin H \cos Az \\ Y_g = X_c \cos H + Y_c \cos Az + Z_c \sin H \sin Az \\ Z_g = -X_c \cos H + Z_c \cos H \end{cases} \quad (A2)$$

where M in the magnetization intensity, H is the core hade (the complement of the dip angle), Az is the core azimuth, I_c is the magnetization inclination in core coordinates, D_c is the magnetization declination in core coordinates, I_g is the magnetization inclination in geographic coordinates, and D_g is the magnetization declination in geographic coordinates.

[40] We ultimately seek I_g and D_g and, therefore, X_g , Y_g , and Z_g . As shown by equation (A2), these three components are functions of H , Az , I_c , D_c , and M . Both H and Az are measured in the field and M is known from our laboratory measurements of each sample. I_c is obtained from the measured vertical component Z_c and $(X_c^2 + Y_c^2)^{1/2}$, which are the only two variables that are independent of the rotations between core segments. The main difficulty is that D_c (and X_c and Y_c) are unknown at depth because of rotation of the core segments. Because the bottom of the first segments of each core (which were absolutely oriented) had magnetization directions I_g , D_g close to that specified by the 2 Ga pole for the melt rocks, and because D_c is approximately constant throughout the core, we arbitrarily chose D_c for each segment so that D_g remained constant from one core segment to the next, propagating down from the top, absolutely oriented segment.

[41] **Acknowledgments.** Helpful reviews were provided by Mike Fuller and an anonymous reviewer. We thank Marco Andreoli for making the thin sections. We thank Eduardo A. Lima, Ian Garrick-Bethell, Jennifer Buz, Joe Kirschvink, Craig Hart, and Jarred Hart for their help during sampling of the cores, and Benjamin Burchfiel for some sample preparation. Geomagnetic surveys were performed with the help of Armand Galdeano, Maxime Le Goff, Manfred Muundjua, and Joshua Gilder. The MPMS XL5 EverCool system at IPGP was financed by the Conseil Régional d’Île-de-France (N°I-06-206/R), INSU-CNRS, IPGP, and ANR (N°06-JCJC-0144). This work was supported by NSF grant EAR-0810244 to

B.P.W., the Victor P. Starr Career Development Professorship, INSU-Dyeti, the French Ministry of Foreign Affairs, the South African National Research Foundation, and DFG SPP Planetar Magnetismus grant GI712-6/1. IPGP contribution 3234.

References

- Appel, P. W. U., N. Abrahamson, and T. M. Rasmussen (2006), Unusual features caused by lightning impact in west Greenland, *Geol. Mag.*, *143*, 737–741, doi:10.1017/S0016756806002391.
- Beard, L. P., et al. (2009), Lightning-induced remanent magnetic anomalies in low-altitude aeromagnetic data, *J. Environ. Eng. Geophys.*, *14*, 155–161.
- Biggin, A. J., et al. (2011), Palaeomagnetism of Archaean rocks of the Onverwacht Group, Barberton Greenstone Belt (southern Africa): Evidence for a stable and potentially reversing geomagnetic field at ca. 3.5 Ga, *Earth Planet. Sci. Lett.*, *302*, 314–328, doi:10.1016/j.epsl.2010.12.024.
- Burke, K., and Y. Gunnell (2008), The African erosion surface: A continental-scale synthesis of geomorphology, tectonics, and environmental change over the past 180 million years, *Mem. Geol. Soc. Am.*, *201*, 1–66.
- Carporzen, L., et al. (2005), Palaeomagnetism of the Vredefort meteorite crater and implications for craters on Mars, *Nature*, *435*, 198–201, doi:10.1038/nature03560.
- Carporzen, L., et al. (2006), Origin and implications of two Verwey transitions in the basement rocks of the Vredefort meteorite crater, South Africa, *Earth Planet. Sci. Lett.*, *251*, 305–317, doi:10.1016/j.epsl.2006.09.013.
- Carter, E. A., et al. (2010), A Raman spectroscopic study of a fulgurite, *Philos. Trans. R. Soc. London, Ser. A*, *368*, 3087–3097, doi:10.1098/rsta.2010.0022.
- Christian, H. J., et al. (2003), Global frequency and distribution of lightning as observed from space by the Optical Transient Detector, *J. Geophys. Res.*, *108*(D1), 4005, doi:10.1029/2002JD002347.
- Cloete, M., et al. (1999), Characterization of magnetite particles in shocked quartz by means of electron- and magnetic force microscopy: Vredefort, South Africa, *Contrib. Mineral. Petrol.*, *137*, 232–245, doi:10.1007/s004100050548.
- Cogné, J. P. (2003), PaleoMac: A Macintosh application for treating paleomagnetic data and making plate reconstructions, *Geochem. Geophys. Geosyst.*, *4*(1), 1007, doi:10.1029/2001GC000227.
- Dunlop, D. J., and O. Ozdemir (1997), *Rock Magnetism: Fundamentals and Frontiers*, 573 pp., Cambridge Univ. Press, New York, doi:10.1017/CBO9780511612794.
- Essene, E. J., and D. C. Fisher (1986), Lightning strike fusion: Extreme reduction and metal-silicate liquid immiscibility, *Science*, *234*, 189–193, doi:10.1126/science.234.4773.189.
- Fisher, R. A. (1953), Dispersion on a sphere, *Proc. R. Soc. London, Ser. A*, *217*, 295–305, doi:10.1098/rspa.1953.0064.
- Frenzel, G., et al. (1989), Stoßwellenmetamorphose, Aufschmelzung und Verdampfung bei Fulguritbildung an exponierten Berggipfeln, *Chem. Erde*, *49*, 265–286.
- Gattacceca, J., and P. Rochette (2004), Toward a robust normalized magnetic paleointensity method applied to meteorites, *Earth Planet. Sci. Lett.*, *227*, 377–393, doi:10.1016/j.epsl.2004.09.013.
- Gibson, R. L. (2002), Impact-induced melting of Archaean granulites in the Vredefort Dome, South Africa. I: Anatexis of metapelitic granulites, *J. Metamorph. Geol.*, *20*, 57–70, doi:10.1046/j.0263-4929.2001.00358.x.
- Gibson, R. L., and W. U. Reimold (2002), *The Vredefort Impact Structure, South Africa: The Scientific Evidence and a Two-Day Excursion Guide*, 111 pp., Counc. Geosci., Pretoria.
- Gibson, R. L., and W. U. Reimold (2005), Shock pressure distribution in the Vredefort impact structure, South Africa, *Spec. Pap. Geol. Soc. Am.*, *384*, 329–349.
- Gill, T. (2008), Initial steps in the development of a comprehensive lightning climatology of South Africa, MSc thesis, 121 pp., Univ. of the Witwatersrand, Johannesburg, South Africa.
- Graham, K. W. T. (1961), The re-magnetization of a surface outcrop by lightning currents, *Geophys. J. Int.*, *6*, 85–102, doi:10.1111/j.1365-246X.1961.tb02963.x.
- Grieve, R. A. F., et al. (1996), Shock metamorphism of quartz in nature and experiment: II. Significance in geoscience, *Meteoritics*, *31*, 6–35.
- Hargraves, R. B. (1970), Paleomagnetic evidence relevant to the origin of the Vredefort ring, *J. Geol.*, *78*, 253–263, doi:10.1086/627516.
- Hart, R. J., et al. (1990), Ultramafic rocks in the center of the Vredefort structure (South Africa): Possible exposure of the upper mantle?, *Chem. Geol.*, *83*, 233–248, doi:10.1016/0009-2541(90)90282-C.
- Hart, R. J., et al. (1995), Magnetic anomaly near the center of the Vredefort structure: Implications for impact-related magnetic signatures, *Geology*, *23*, 277–280, doi:10.1130/0091-7613(1995)023<0277:MANTCO>2.3.CO;2.
- Hart, R. J., et al. (1999), Archean age for the granulite facies metamorphism near the center of the Vredefort structure, South Africa, *Geology*, *27*, 1091–1094, doi:10.1130/0091-7613(1999)027<1091:AAFTGF>2.3.CO;2.
- Hart, R. J., et al. (2000), “Super magnetic” rocks generated by shock metamorphism from the centre of the Vredefort impact structure, South Africa, *S. Afr. J. Geol.*, *103*, 151–155, doi:10.2113/103.2.151.
- Hart, R. J., et al. (2004), New PGE and Re/Os-isotope data from lower crustal sections of the Vredefort Dome and a reinterpretation of its “crust on edge” profile, *S. Afr. J. Geol.*, *107*, 83–94.
- Henkel, H., and W. U. Reimold (1998), Integrated geophysical modelling of a giant, complex impact structure: Anatomy of the Vredefort structure, South Africa, *Tectonophysics*, *287*, 1–20, doi:10.1016/S0040-1951(98)80058-9.
- Henkel, H., and W. U. Reimold (2002), Magnetic model of the central uplift of the Vredefort impact structure, South Africa, *J. Appl. Geophys.*, *51*, 43–62, doi:10.1016/S0926-9851(02)00214-8.
- Hood, L. L., and N. A. Artemieva (2008), Antipodal effects of lunar basin-forming impacts: Initial 3D simulations and comparisons with observations, *Icarus*, *193*, 485–502, doi:10.1016/j.icarus.2007.08.023.
- Huebner, J. S., and R. G. Dillenburg (1995), Impedance spectra of hot, dry silicate minerals and rock: Qualitative interpretation of spectra, *Am. Mineral.*, *80*, 46–64.
- Jackson, G. M. (1982), Paleomagnetic study and magnetic modeling of the Vredefort dome, BSc honors thesis, 46 pp., Univ. of the Witwatersrand, Johannesburg, South Africa.
- Jones, B. E., et al. (2005), Oxide reduction during triggered-lightning fulgurite formation, *J. Atmos. Sol. Terr. Phys.*, *67*, 423–428, doi:10.1016/j.jastp.2004.11.005.
- Kamo, S. L., et al. (1996), A 2.023 Ga age for the Vredefort impact event and a first report of shock metamorphosed zircons in pseudotachylitic breccias and granophyre, *Earth Planet. Sci. Lett.*, *144*, 369–387, doi:10.1016/S0012-821X(96)00180-X.
- Kirschvink, J. L. (1980), The least-squares line and plane and the analysis of paleomagnetic data: Examples from Siberia and Morocco, *Geophys. J. R. Astron. Soc.*, *62*, 699–718.
- Kirschvink, J. L., R. E. Kopp, T. D. Raub, C. T. Baumgartner, and J. W. Holt (2008), Rapid, precise, and high-sensitivity acquisition of paleomagnetic and rock-magnetic data: Development of a low-noise automatic sample changing system for superconducting rock magnetometers, *Geochem. Geophys. Geosyst.*, *9*, Q05Y01, doi:10.1029/2007GC001856.
- Kletetschka, G., et al. (2004), An empirical scaling law for acquisition of the thermoremanent magnetization, *Earth Planet. Sci. Lett.*, *226*, 521–528, doi:10.1016/j.epsl.2004.08.001.
- Koerberl, C., et al. (1996), Re-Os isotope and geochemical study of the Vredefort Granophyre: Clues to the origin of the Vredefort structure, South Africa, *Geology*, *24*, 913–916, doi:10.1130/0091-7613(1996)024<0913:ROIAGS>2.3.CO;2.
- Macouin, M., et al. (2004), Long-term evolution of the geomagnetic dipole moment, *Phys. Earth Planet. Inter.*, *147*, 239–246, doi:10.1016/j.pepi.2004.07.003.
- Maki, D. (2005), Lightning strikes and prehistoric ovens: Determining the source of magnetic anomalies using techniques of environmental magnetism, *Geoarchaeology Int. J.*, *20*, 449–459.
- Malki, M., and P. Echegut (2003), Electrical conductivity of the CaO-SiO₂ system in the solid and the molten states, *J. Non Cryst. Solids*, *323*, 131–136, doi:10.1016/S0022-3093(03)00298-9.
- McFadden, P. L., and A. B. Reid (1982), Analysis of palaeomagnetic inclination data, *Geophys. J. R. Astron. Soc.*, *69*, 307–319.
- Moser, D. E., et al. (2001), Birth of the Kaapvaal tectosphere 3.08 billion years ago, *Science*, *291*, 465–468, doi:10.1126/science.291.5503.465.
- Muundjua, M., et al. (2007), Magnetic imaging of the Vredefort impact crater, South Africa, *Earth Planet. Sci. Lett.*, *261*, 456–468, doi:10.1016/j.epsl.2007.07.044.
- Nakamura, N., K. Okuno, M. Uehara, T. Ozawa, L. Tatsumi-Petrocholis, and M. Fuller (2010), Coarse-grained magnetites in biotite as a possible stable remanence-carrying phase in Vredefort granites, *Geol. Soc. Am. Spec. Pap.*, *465*, 165–172.
- Nel, L. T. (1927), Geological map of the country around Vredefort, scale 1:63360, *Union of S. Afr.*, Dep. of Mines and Ind., Geol. Surv., Pretoria.
- Özdemir, Ö., D. J. Dunlop, and B. M. Moskowitz (1993), The effect of oxidation on the Verwey transition in magnetite, *Geophys. Res. Lett.*, *20*, 1671–1674, doi:10.1029/93GL01483.
- Perchuk, L. L., et al. (2002), Dynamic and thermal history of the Vredefort explosion structure in the Kaapvaal craton, South Africa, *Petrologiya*, *10*, 451–492.

- Reimold, W. U., and R. L. Gibson (1996), Geology and evolution of the Vredefort impact structure, South Africa, *J. Afr. Earth Sci.*, *23*, 125–162, doi:10.1016/S0899-5362(96)00059-0.
- Sakai, H., et al. (1998), Study of lightning current by remanent magnetization, *Electr. Eng. Jpn.*, *123*, 41–47, doi:10.1002/(SICI)1520-6416(199806)123:4<41::AID-EEJ6>3.0.CO;2-O.
- Salminen, J., et al. (2009), Paleomagnetic and rock magnetic study of the Vredefort impact structure and the Johannesburg Dome, Kaapvaal Craton, South Africa—Implications for the apparent polar wander path of the Kaapvaal craton during the Mesoproterozoic, *Precambrian Res.*, *168*, 167–184, doi:10.1016/j.precamres.2008.09.005.
- Shimizu, H., et al. (2007), A geomagnetic total intensity anomaly originated from lightning-induced isothermal remanent magnetization: Case of the Yatsugatake Magnetic Observatory, central Japan, *Earth Planets Space*, *59*, 141–149.
- Slawson, W. F. (1976), Vredefort core: A cross-section of the upper crust?, *Geochim. Cosmochim. Acta*, *40*, 117–121, doi:10.1016/0016-7037(76)90199-X.
- Strik, G., T. S. Blake, T. E. Zegers, S. H. White, and C. G. Langereis (2003), Palaeomagnetism of flood basalts in the Pilbara Craton, Western Australia: Late Archaean continental drift and the oldest known reversal of the geomagnetic field, *J. Geophys. Res.*, *108*(B12), 2551, doi:10.1029/2003JB002475.
- Tauxe, L., C. Constable, C. L. Johnson, A. A. P. Koppers, W. R. Miller, and H. Staudigel (2003), Paleomagnetism of the southwestern U.S.A. recorded by 0–5 Ma igneous rocks, *Geochem. Geophys. Geosyst.*, *4*(4), 8802, doi:10.1029/2002GC000343.
- Tredoux, M., C. Constable, C. L. Johnson, A. A. P. Koppers, W. R. Miller, and H. Staudigel (1999), Ultramafic rocks at the center of the Vredefort structure: Further evidence for the crust on edge model, *Geology*, *27*, 923–926, doi:10.1130/0091-7613(1999)027<0923:URATCO>2.3.CO;2.
- van Velzen, A. J., and J. D. A. Zijdeveld (1995), Effects of weathering on single-domain magnetite in Early Pliocene marine marls, *Geophys. J. Int.*, *121*, 267–278, doi:10.1111/j.1365-246X.1995.tb03526.x.
- Verrier, V., and P. Rochette (2002), Estimating peak currents at ground lightning impacts using remanent magnetization, *Geophys. Res. Lett.*, *29*(18), 1867, doi:10.1029/2002GL015207.
- Weiss, B. P., J. Gattacceca, S. Stanley, P. Rochette, and U. R. Christensen (2010), Paleomagnetic records of meteorites and early planetesimal differentiation, *Space Sci. Rev.*, *152*, 341–390, doi:10.1007/s11214-009-9580-z.

L. Carporzen, Équipe de paléomagnétisme, Institut de Physique du Globe de Paris, Sorbonne Paris Cité, University of Paris VII -Denis Diderot, UMR 7154 CNRS, 1 rue Jussieu, Paris F-75005, France. (lcarpo@ipggp.fr)

S. A. Gilder, Department of Earth and Environmental Sciences, Ludwig Maximilians University, D-80333 Munich, Germany.

R. J. Hart, iThemba Labs, Private Bag 11 WITS, Johannesburg 2050, South Africa.

A. Pommier, School of Earth and Space Exploration, Arizona State University, Tempe, AZ 85287, USA.

B. P. Weiss, Department of Earth, Atmospheric, and Planetary Sciences, Massachusetts Institute of Technology, Cambridge, MA 02139, USA.